



MHD Flow Darcy Forchheimer of Jeffrey Nanofluid over a Stretching Sheet Considering Melting Heat Transfer and Viscous Dissipation

Naresh Kumar¹, Gandrakota Srinivasu¹, Balagnoor Srikantha setty², Mani Ramanuja^{2,*}

¹ Department of Mathematics, Institute of Aeronautical Engineering, Dundigal, Hyderabad – 500 043, India

² Department of Mathematics, Marri Laxman Reddy Institute of Technology and Management, Dundigal, Hyderabad – 500 043, India

ARTICLE INFO

Article history:

Received 6 August 2023

Received in revised form 9 September 2023

Accepted 12 October 2023

Available online 21 January 2024

Keywords:

MHD; Jeffrey nanofluid; Darcy number; Deborah number; Melting parameter

ABSTRACT

This work investigates the MHD flow of a Jeffrey nanofluid through a non-linear stretching sheet, considering melting heat transfer and the combined influences of concentration and thermal radiation. A variable magnetic effect normal to the flow direction is enforced to reinforce the conductivity of the Jeffrey nanofluid. The governing non-linear PDEs with convective boundary conditions are transformed into the non-dimensional ODEs, and we apply appropriate similarity variables. The further similarity transformation is determined with the 4th-order Runge-Kutta shooting technique facilitated. The approach is implemented for convergent relations of the rate field, temperature, and nano-particle concentration. However, small magnetic Reynolds is considered to decline the induced magnetic impact. Melting parameter enhances temperature and concentration. Finally, the effect of fluid parameters such as thermophoresis, melting parameter, Deborah number, chemical reaction, Brownian motion, inertia parameter, Darcy number, and thermophoresis on the MHD flow profiles is examined graphically.

1. Introduction

Rapid advancement in several domains of technology and science has pressed academics to broaden their study to comprise the regime of boundary layer flow over a stretched sheet. Rubber sheet manufacturing, Metal spinning, glass fiber production, petroleum industries extrusion of polymer sheets, glass fabrication materials operations, high-temperature plasmas, polymer processing, and liquid metamaterials are just a few of the manufacturing and production processes where boundary layer flow behavior in the direction of a linearly or non-linearly stretching sheet plays an essential task in solving engineering trouble, etc. At a soaring temperature, thermal radiation changes the boundary sheet's temperature distribution, influencing the wall's heat transfer.

Non-Newtonian fluid dynamics is a popular area of research for the investigation. Recent researchers have paid deep attention to this field of study due to its use in industry and many other fields. A single constitutive equation can elaborate the viscous fluids, whereas a single constitutive expression cannot debate non-Newtonian fluids due to their different structures. Therefore,

* Corresponding author.

E-mail address: mramanuja09@gmail.com (Mani Ramanuja)

<https://doi.org/10.37934/cfdl.16.6.131145>

numerous models of non-Newtonian materials exist. In the past, much attention was devoted to subclasses of differential and rate-type liquids. Jeffrey material is one of the non-Newtonian liquids which can predict the retardation and relaxation effects. Due to its application in bio-engineering, geophysics, oil reservoir processes, and chemical and nuclear technologies, the Jeffrey fluid model has remarkable importance.

Lee [1] and Narain *et al.*, [2] looked at the flow behavior of Jeffrey fluid due to the non-linear surface stretching in the radial direction. Further, they were the first to explore boundary layer improvement near a thin needle in a viscous fluid. Sakiadis [3] investigation of boundary layer flow and heat exchange via a stretching surface has drawn the thought of various specialists. Hayat *et al.*, [4] and Akbar *et al.*, [5] have explored the flow of an Eyring–Powell non-Newtonian fluid across a moving surface with convective boundary conditions. And also across a stretched sheet and the impacts of the heating system and mass transfer on the peristaltic flow. However, to our awareness, no attempt has been made to analyze Eyring–Powell fluid across an exponentially diminishing sheet. Mabood *et al.*, [6] inspected the numerical investigation of magneto-hydrodynamic (MHD) nano-fluids with chemical reactions. Consequently, chemical reaction inflows of pseudo-plastic nano-fluid over channel were revealed by Hayat *et al.*, [7], which examined numerical results of chemical reactions in Williamson nano-fluids due to the stretching. Suggested, Krishnamurthy *et al.*, [8] and Hayat *et al.*, [9] analytical research of chemically reactive Maxwell nano-fluid flows across the bidirectional surface.

The melting phenomena are widely used in technologies; researchers have carefully considered making more effective, sustainable, and energy-efficient technologies. Excess heat repossession, planetary power, and plant heat are all linked by such technologies. Three processes have been implemented for energy storage: latent, sensible heat, and chemical energy. Latent heat is a cost-effective way to store heat energy by adjusting the material phase. The thermal energy is ejected by latent heat, i.e., melting, and regained by freezing in hydraulic processes. The melting phenomena are used in various applications, including heat exchanger coils, freeze treatment-based pumps, solidification, welding operations, etc., and many others studied by Hayat *et al.*, [10], Roberts *et al.*, [11], Rahman *et al.*, [12], Das *et al.*, [13], and Hayat *et al.*, [14].

The use of nanofluid creates these conditions, which increase the rate of heat transmission. Grosan *et al.*, [15] have investigated forced convection flow over a thin needle with a changing surface temperature. Trimbitas *et al.*, [16] Hayat *et al.*, [17] and Ahmad *et al.*, [18] have published a collection of boundary layer flow through a thin needle with varied physical influences in a nanofluid. Furthermore, MHD flows via a moving vertical slender needle in nanofluid via Buongiorno's form with the boundary situation. Furthermore, Majdalani *et al.*, [19] have offered a numerical and analytical solution for viscous fluid flow via a contracting permeable channel. Furthermore, they have published an analytical approach for micro-polar fluid flow in a porous medium. Fakour *et al.*, [20], Hatami *et al.*, [21] and Hady *et al.*, [22] have used porous fins to explore laminar nanofluid flow in a semi-porous channel with a magnetic field influence of heat and mass transfer analysis.

The unsteady flow, mass, and heat transfer study for nanofluids via a contracting cylinder was explored by Zaimi *et al.*, [23]. Chen [24] studied how vicious and joule effects affected the convective and radiative flow models. In the presence of gyrotactic microorganisms and nano-particles, Khan *et al.*, [25] explored numerical convection flow. Jaber *et al.*, [26] looked into the numerical results of a viscous fluid moving across a horizontal plate under a power-law thermal condition. Because of its vast mechanical and industrial applications in industry metallurgical procedures, fiber, copper wires tinning, assembling of plastic, and plastic sheets. Further, Rasool *et al.*, [27] have established the heat and mass transfer developments in boundary layer Jeffery nanofluid flow across a stretched surface

using the Darcy-Forchheimer relation. Mani *et al.*, [28] have studied the effect of chemically reactive nanofluid flowing across horizontal cylinders by using numerical Solutions.

Lim Yeou *et al.*, [29] inspected, the high thermal conductivity of titanium dioxide (TiO_2) makes it ideal for heat transfer, particularly in a solar collector. However, nanofluids containing dissolved nanoparticles tend to agglomerate. Shahirah Abu *et al.*, [30] have investigated the mixed convection boundary layer flow over a permeable surface embedded in a porous medium, filled with a nanofluid, and subjected to thermal radiation, magnetohydrodynamics (MHD), and internal heat generation. Akshay Ranjan *et al.*, [31] study of the structural response of the tank. The design of a composite liner-less tank is determined by the strain's transverse to the direction of the fibers, and the tank must be able to contain the pressurized fluid without leakage under all given loading conditions. Mostafa *et al.*, [32] have examined the activation of MNPs for hyperthermia therapy via an external alternating magnetic field, which is an interesting method in targeted cancer therapy. Mani and Gopi [33] study the entropy analysis of MHD flow of Jeffrey fluid in an inclined channel. Mani *et al.*, [34] have examined the effect of chemically reative nanofluid flowing across horizontal cylinder.

Inspired by the exceeding investigation, in the current work, we examined the Darcy forchheimer of Jeffrey nano-fluid MHD flow and heat transfer via a non-linear stretching sheet considering melting heat transfer and viscous dissipation. The solution of coupled non-linear PDE's into nondimensional ODE's is obtained numerically by using the shooting technique coupled with the 4th order Runge-Kutta technique (MATLAB solver, bvp4c package software). The contribution of various model factors comprising present work and previsions work and also. This work is concerned about constant numerical results, which are investigated graphically and discussed quantitatively concerning the effects of several parameters, such as the Radiation parameter, Magnetic parameter, Thermopherasis, Brownian motion parameter, Darcy number, Deborah number, and shape parameter.

Several important engineering variables are also given, such as skin friction coefficient, local Sherwood number, and local Nusselt number. The findings of this revise may be used to manage the heat transit and fluid rate in any manufacturing process or industrial application to achieve the required end-product quality.

2. Methodology

2.1 Mathematical Formulation of the Model

The present analysis considers $2-D$ incompressible MHD Jeffrey nanofluid fluid flow over a non-linearly stretching sheet. Linear behavior generates flow, and the sheet is stretched in both directions of the x -axis with stretching sheet $U_w = a_1(x+b_1)^n$ velocity, whereas x denotes a_1 and b_1 constant and stretching surface co-ordinate, respectively. In the present study represents Figure 1 as the physical form. The incompressible nanofluid boundary layer flow's continuity, momentum, energy, and concentration [9] are below:

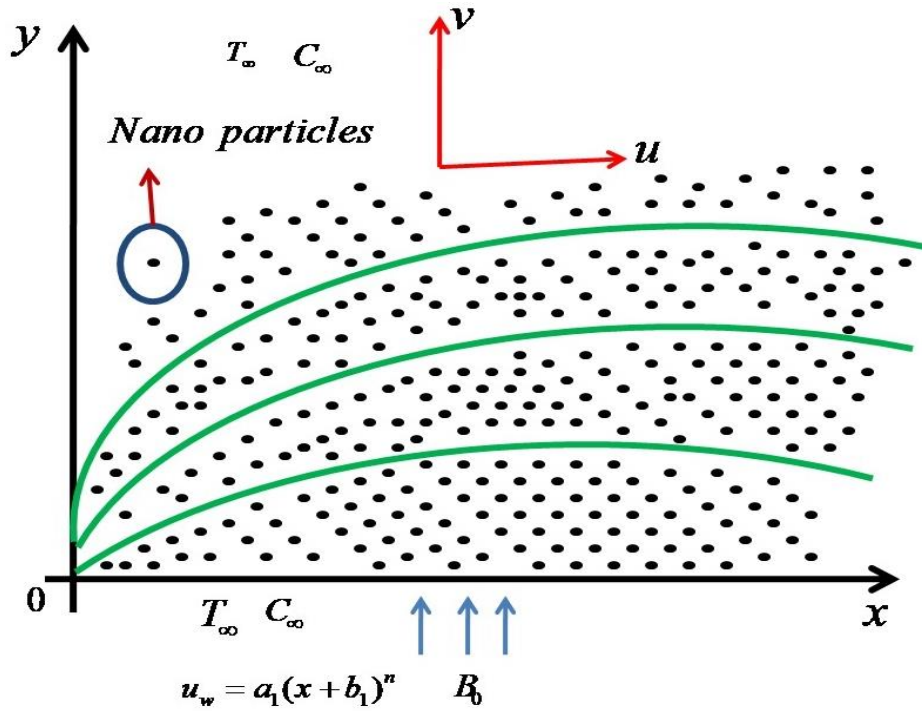


Fig. 1. Physical modal of the problem

$$\frac{\partial u}{\partial x} + \frac{\partial v}{\partial y} = 0 \quad (1)$$

$$u \frac{\partial u}{\partial x} + v \frac{\partial u}{\partial y} = \frac{\nu}{(1+\lambda_s)} \left[\frac{\partial^2 u}{\partial y^2} + \lambda_t \left(v \frac{\partial^3 u}{\partial y^3} + u \frac{\partial^3 u}{\partial x \partial y^2} - \frac{\partial u}{\partial x} \frac{\partial^2 u}{\partial y^2} + \frac{\partial^2 u}{\partial x \partial y} \frac{\partial u}{\partial y} \right) \right] - \left(\frac{\sigma B_0^2}{\rho} + \frac{\nu \varepsilon}{k} \right) u - \frac{c_b \varepsilon}{\sqrt{k}} u^2 \quad (2)$$

$$u \frac{\partial T}{\partial x} + v \frac{\partial T}{\partial y} = \tau \left[\frac{D_T}{T_\infty} \left(\frac{\partial T}{\partial y} \right)^2 + D_B \frac{\partial C}{\partial y} \frac{\partial T}{\partial y} \right] + \alpha \frac{\partial^2 T}{\partial y^2} + \frac{16\sigma^* T_\infty^3}{3k^* \rho c_p} \frac{\partial^2 T}{\partial y^2} + \frac{Q_0(T_0 - T_m)}{(\rho c)_p} \quad (3)$$

$$u \frac{\partial C}{\partial x} + v \frac{\partial C}{\partial y} = \frac{D_T}{T_\infty} \frac{\partial^2 T}{\partial y^2} + D_B \frac{\partial^2 C}{\partial y^2} - K_n (C - C_w)^m \quad (4)$$

The boundary situations at the surface of the sheet and far from it are written as:

$$u = u_w(x) = a_0(x+b_0)^n, T = T_w, C = C_w, v = 0, \quad (5)$$

$$\text{at } y = \delta(x+b_0)^{(1-n)/2}$$

$$u \rightarrow 0, \text{ as } y \rightarrow \infty, T \rightarrow T_\infty, C \rightarrow C_\infty \quad (6)$$

By introducing the following non-dimensional variables are [9];

$$\begin{aligned} \psi(x, y) &= \sqrt{\frac{2\nu a_0}{1+n}} (x+b_0)^{n+1} f(\eta), \quad \eta = \sqrt{\frac{(n+1)a_0}{2\nu}} (x+b_0)^{n-1} y, \\ u &= a_0(x+b_0)^n f'(\eta), \quad v = -\sqrt{\frac{\nu(n+1)}{2}} a_0(x+b_0)^{n-1} \left[f(\eta) + \eta \left(\frac{n-1}{n+1} \right) f'(\eta) \right] \\ \theta(\eta) &= \frac{T-T_w}{T-T_\infty}, \quad \phi(\eta) = \frac{C-C_w}{C_w-C_\infty} \end{aligned} \quad (7)$$

Now, using Eq. (5) and Eq. (7) the non-dimensional form of the leading Eq. (2)-(4) are expressed as

$$\begin{aligned} f''' - K \left[\left(\frac{1+n}{2} \right) f f^{iv} - (n-1) f f''' - \left(\frac{3n-1}{2} \right) f'^2 \right] - \left(\frac{2n}{n+1} \right) (1+\lambda_s) f'^2 \\ - \left(\frac{2}{n+1} \right) (1+\lambda_s) [Mf' - \beta f'^2 - (Da)f'] = 0 \end{aligned} \quad (8)$$

$$\frac{1}{Pr} \left(1 + \frac{4}{3} R \right) \theta'' + f\theta' + Nt(\theta')^2 + Nb\theta'\phi' + \frac{2}{n+1} \lambda\theta = 0 \quad (9)$$

$$\phi'' + Pr Le f\phi' + \frac{Nt}{Nb} \theta'' + \Gamma\phi^m = 0 \quad (10)$$

Similarity the non-dimensional boundary situations are [9];

$$f(0) = 0, \quad f'(0) = 1, \quad \theta(0) = 1, \quad \phi(0) = 0 \quad \text{at } \eta = 0 \quad (11)$$

$$f'(\infty) \rightarrow 0, \quad \theta(\infty) \rightarrow 0, \quad \phi(\infty) \rightarrow 0 \quad \text{at } \eta \rightarrow 0 \quad (12)$$

These parameters have the following values

$$\begin{aligned} M &= \sqrt{(\sigma / \rho a)} B_0, \quad Pr = \frac{\nu}{\alpha}, \quad Le = \frac{\alpha}{D_B}, \quad Da = \frac{\varepsilon \nu}{ka_0(x+b_0)^{n-1}}, \quad Nt = \frac{\tau D_T (T_w - T_\infty)}{T_\infty \nu}, \\ Nb &= \frac{\tau D_B (c_w - c_\infty)}{\nu}, \quad H = \frac{Q_0}{a \rho c_p}, \quad Me = \frac{C_p (T_w - T_\infty)}{\lambda^* + C_s (T_w - T_0)}, \quad R = \frac{4\sigma^* T_\infty^3}{kk^*}, \\ \beta &= \frac{C_b \varepsilon (x+b_0)}{\sqrt{k}}, \quad \Gamma = K_n x (C_w - C_\infty)^{n-1} \end{aligned} \quad (13)$$

The important of non-dimensional quantities are the skin friction coefficient C_{fx} , the local Nusselt number Nu_x and the Sherwood number Sh_x represented as;

$$Nu_x = \frac{(x+b_0)q_w}{k(T_w - T_\infty)}, C_{fx} = \frac{\tau_w}{1/2\rho u_w^2}, \quad \text{and} \quad Sh_x = \frac{(x+b_0)q_m}{D_B(C_w - C_\infty)} \quad (14)$$

Using Eq. (8) and Eq. (14), the skin friction coefficient the local Nusselt number, and the local Sherwood number can be written as

$$\begin{aligned} \text{Re}^{1/2} C_{fx} &= \frac{1}{1+\lambda_s} \left[f''(0) + K \left(f'(0)f''(0) - \left(\frac{n+1}{2} \right) f(0)f'''(0) \right) \right], \\ \text{Re}^{-1/2} Nu_x &= -(1+R)\sqrt{\frac{1+n}{2}}\theta'(0), \quad \text{Re}_x^{-1/2} Sh_x = -\sqrt{\frac{1+n}{2}}\phi'(0) \end{aligned} \quad (15)$$

Where Re is the local Reynolds number $\text{Re} = \frac{(x+b_0)^{n+1}a_0}{\nu}$ based on the stretching rate.

3. Results

3.1 Results and Discussion

In this paper, we have examined the combined influences of darcy forchheimer of MHD Jeffrey nano-fluid flow and heat transfer via a non-linear stretching sheet considering melting heat transfer and viscous dissipation is investigated the governing Eq. (8), Eq. (9) and Eq. (10) with boundary situation Eq. (11) and Eq. (12) were numerically by using the 4th order Runge-Kutta scheme with shooting system. The rate and temperature profiles (2) to (20) are examined with the presence of the magnetic field.

For evaluating the consistency and accuracy of our accurate solutions numerical results of the significant parameters are lighted through graphs in this section. We were conceded out by computations taken $1.2 \leq R \leq 1.8$, $0.12 \leq Nt \leq 0.96$, $0.4 \leq n \leq 1.6$, $0.10 \leq M \leq 1.74$, $0.4 \leq k \leq 1.6$, $0.22 \leq Da \leq 0.88$, $0.4 \leq \Gamma \leq 1.6$, $1 \leq \beta \leq 4$, $1.2 \leq \beta_s \leq 4.8$. Numerical simulations are used to get the findings, which take into account several non-dimensional controlling parameters impact of parameters such as Radiation parameter R , Magnetic parameter M , Thermophoreses Nt , Brownian motion parameter Nb , Darcy number Da , Deborah number k , shape parameter n . We secure the values of non-dimensional variables for numerical solutions R .

Figure 2 interprets the significance of radiation parameter R on temperature profiles; we can notice that radiation enhances the fluid temperature over the stretching sheet. The radiation parameter R specifies how much conduction heat transfer contributes to thermal radiation transfer. A rise in the radiation parameter thus in increasing temperature within the boundary layer of the stretching sheet. Figure 3 shows the impact of thermophoresis with a concentration of nano-fluid. We noticed the inverse effect in this case generation due to a temperature gradient's formation, which resulted from the mixing of different molecular specie. The concentration in the field enhances by increasing the value of the (Nt) thermophoresis parameter because concentration boundary layer thickness is a diminishing function within the boundary layer of the stretching sheet. Figure 4

illustrates the effects of shape parameter n on the concentration of nanofluid flow in a stretching sheet. We noticed that the nanofluid concentration enhances, and the shape parameter n decreases in the case of heat generation/absorption within the boundary layer of the stretching sheet. Figure 5. Displays the impact of shape parameter n on the temperature of a nano-fluid in a stretching sheet. We observed that the shape parameter n decreases with the temperature of nano-fluid over a stretching sheet. Figure 6 display the impact of thermophoresis on concentration nano-particles. Thus the width of the boundary layer, we observed that the thermophoresis parameter increases and concentration enhance as well in the case of heat generation. As a result, we may deduce that boosting the thermophoresis parameter Nt lowered heat and mass exchange. Thermo-phoresis effect in the improvement of the concentration field near the surface.

Figure 7 displays the impact of the magnetic field on velocity. We noticed that the magnetic parameter reduces the rate of the fluid. The cause behind this is the resistive force termed as Lorentz force, which slow down the fluid velocity. That magnetic parameter M is resistance, the Lorentz force is produced, and this magnetic characteristic may be used to regulate fluid flow. As a result, raising the value of the magnetic parameter leads the rate distribution to decline. Depict the melting parameter on temperature influence shown in the Figure 8. The temperature of nanofluid increases flow in the stretching sheet, then the melting parameter also enhances. Concentration is higher in the presence of melting. Figure 9 indicates the influence of melting parameter on the concentration of nanofluid flow in a stretching sheet. The melting parameter is found to enhance the engagement for both stretching and shrinking sheet. Figure 10 illustrates the plots for Deborah number K on temperature Jeffery nano-fluid; we noticed that the Deborah number enhances the temperature increases on the starching sheet due to temperature to extrapolate temperature-dependent mechanical properties of polymers.

Figure 11 shows that the influence of Deborah number k on the concentration of nanofluid flow in the stretching sheet. We noticed that the Deborah number k increases the concentration of nanofluid enhances due the leads to diminish in the momentum boundary layer thickness and an enhance in the thermal boundary layer thickness. Figure 12 illustrate that the impact of Darcy Da on the flow velocity of the nanofluid stretching sheet. We observed that the Da Darcy number enhances and the rate of fluid decrease. Figure 13 interprets that to explore the influences of Darcy's number Da on flow and temperature distributions. It is noticed that enhances Darcy number Da values velocity up the motion of fluid particles but the temperature of fluid decreases near the stretching sheet. The effect of Darcy's number Da on the concentration nanofluid flow on stretching sheet profile Figure 14. Concentration nanofluid flow on the stretching sheet enhances Darcy's parameter decreases. It is clear from Figure 15 shows the chemical reaction parameter Γ on the concentration of the nanofluid flow on the stretching sheet. We noticed that the chemical reaction parameter enhances the attention of the nanofluid fluid increases flux distribution near the wall. On the melting surface, the volume fraction of nano-particles falls for constructive chemical reaction parameters Γ and increases for destructive chemical reaction parameters. The melting parameter lowers the temperature field while increasing velocity.

Figure 16 illustrates the impact of the inertia parameter β on temperature on the stretching sheet. We observed that the inertia parameter enhances temperature increase nanofluid fluid flow. It can be observed from Figure 17 that the impact of heat generation β_s on velocity nanofluid nonlinear stretching sheet. We noticed that the nanofluid rate enhances the heat generation parameter in this case. Figure 18 the impact of enhancing the heat absorption/ generation parameter β_s decreases the heat transfer coefficient. Also, during heat creation, the direction of heat transmission is reversed. In the presence of both heat generation and absorption together with the

boundary layer, the thickness of the thermal boundary layer is found to improve. Figure 19 shows heat source generation/ absorption β_s on the concentration of nanofluid flow in a stretching sheet. The concentration of nanofluid decreases in the case of generation and absorption. The influence of the heat source parameter on concentration fluid is reveals in Figure 20. We observed that the heat source enhances the concentration of the fluid. These outlines revealed that fluid concentration layer frequently declined with enhance in the values of parameter β .

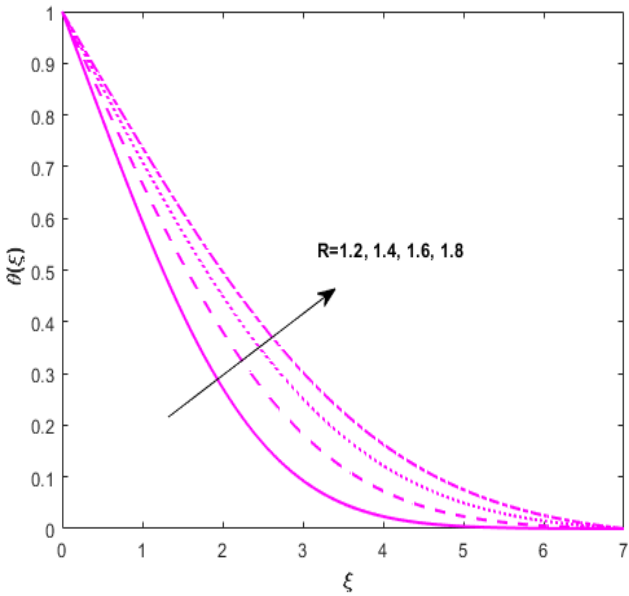


Fig. 2. Depicts the R on $\theta(\xi)$ distribution

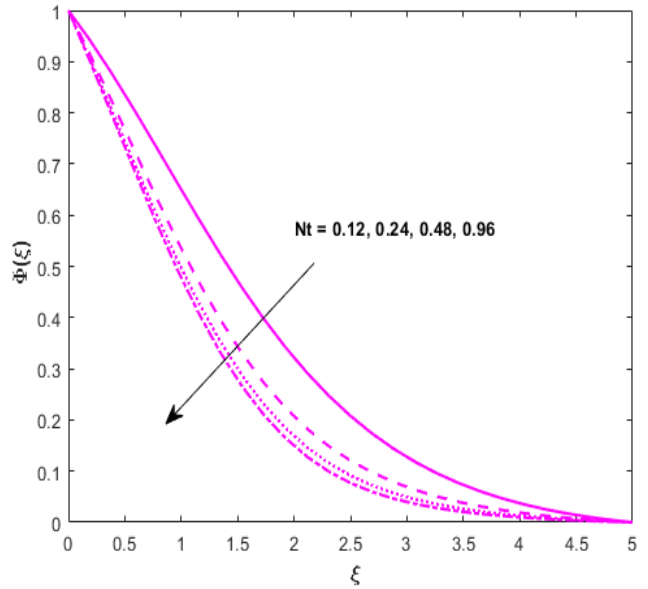


Fig. 3. Depicts the Nt on $\theta(\xi)$ distribution

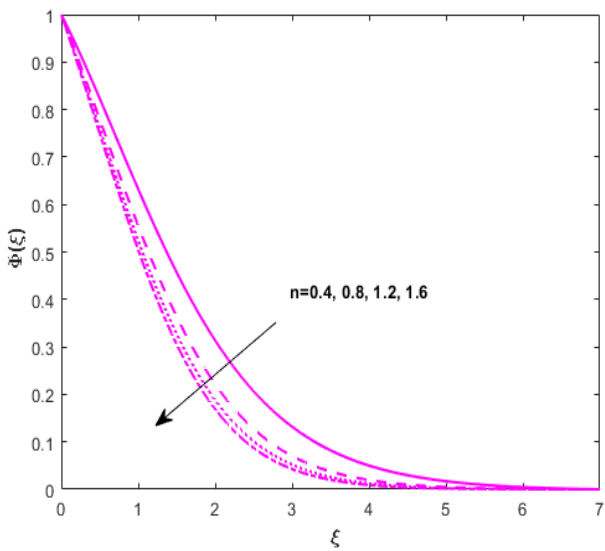


Fig. 4. Depicts the n on $\theta(\xi)$ distribution

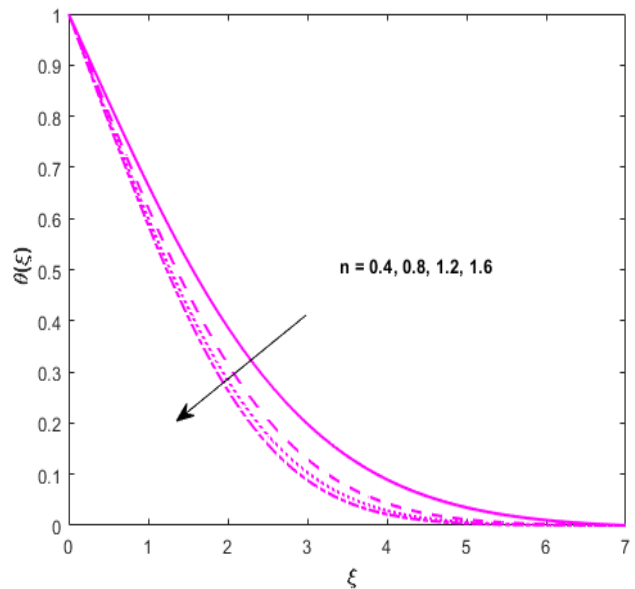


Fig. 5. Depicts the n on $\theta(\xi)$ distribution

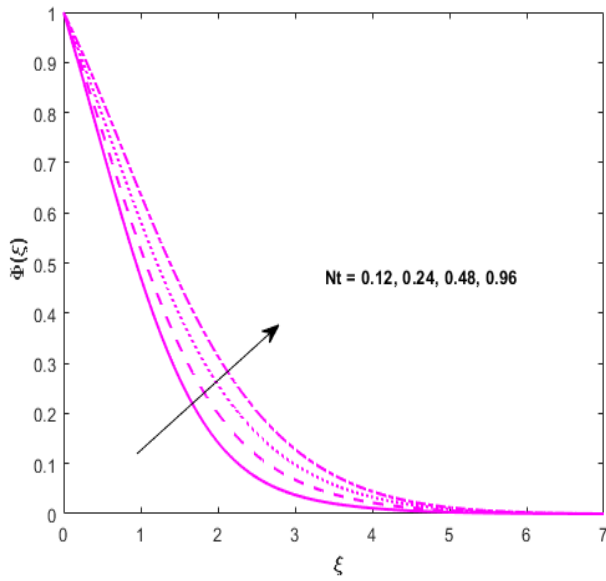


Fig. 6. Depicts the Nt on $\theta(\xi)$ distribution

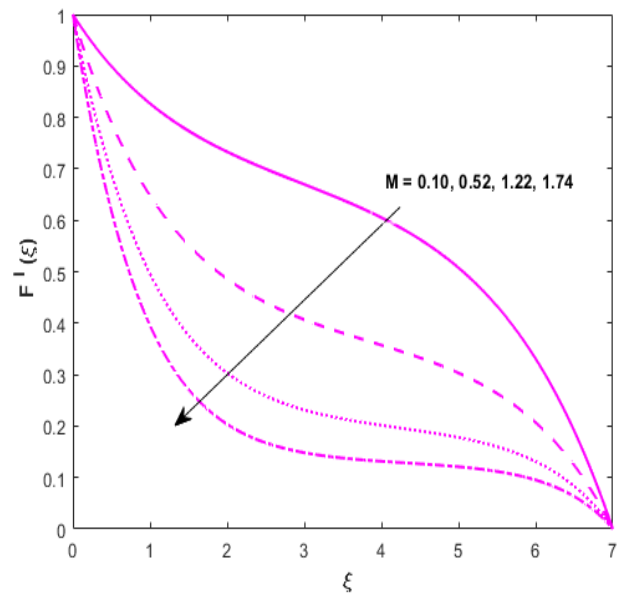


Fig. 7. Depicts the M on $F^I(\xi)$ distribution

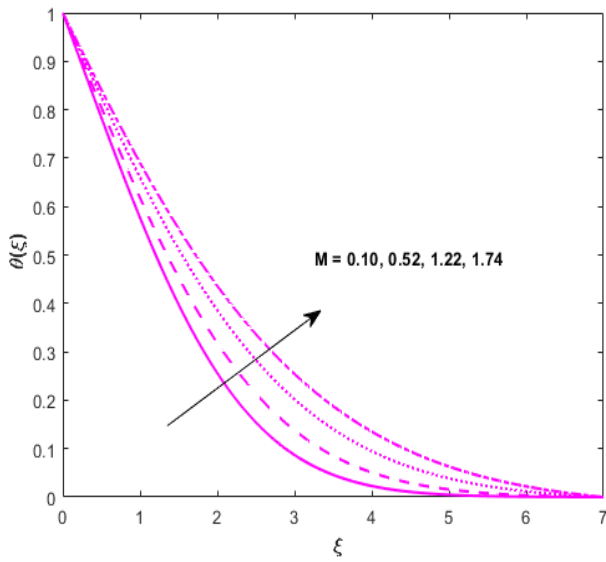


Fig. 8. Depicts the M on $\theta(\xi)$ distribution

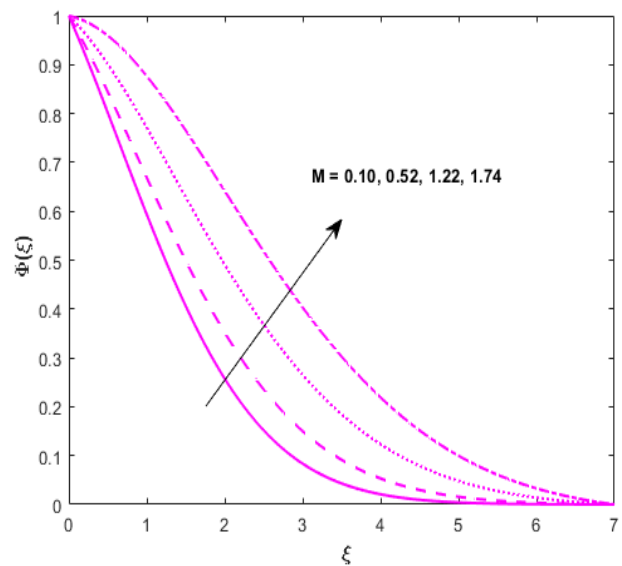


Fig. 9. Depicts the M on $\theta(\xi)$ distribution

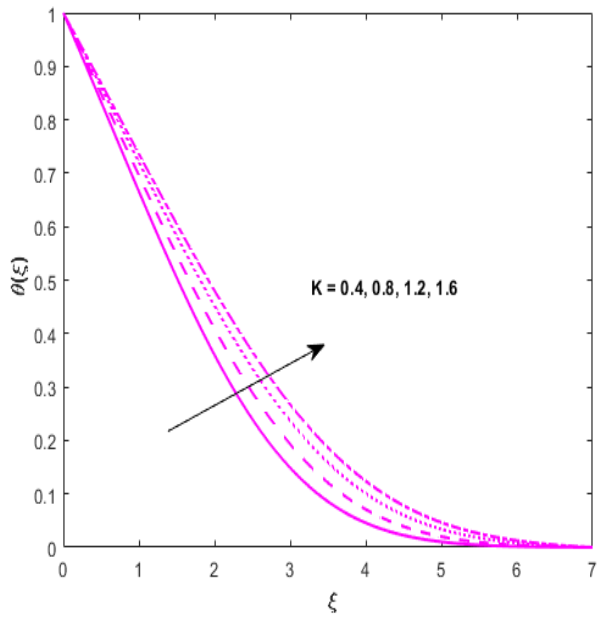


Fig. 10. Depicts the k on $\phi(\xi)$ distribution

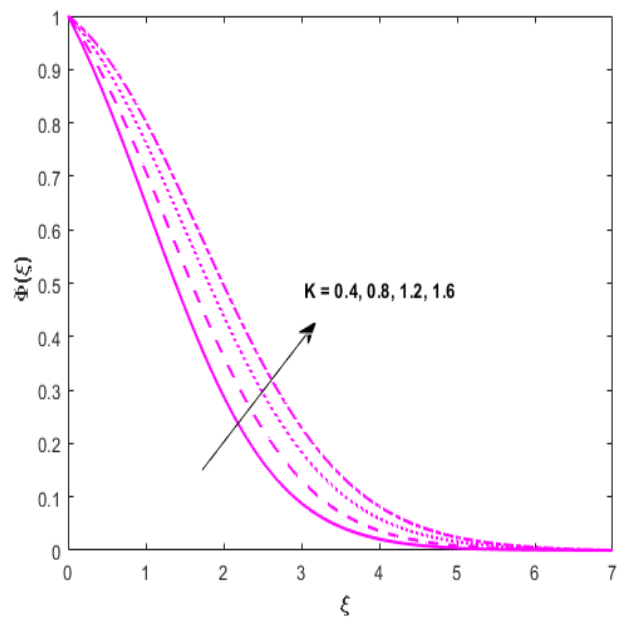


Fig. 11. Depicts the k on $\phi(\xi)$ distribution

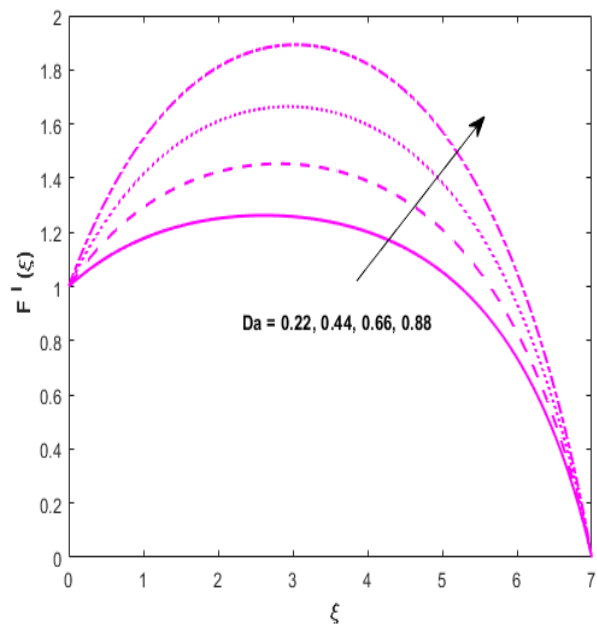


Fig. 12. Depicts the Da on $F'(\xi)$ distribution

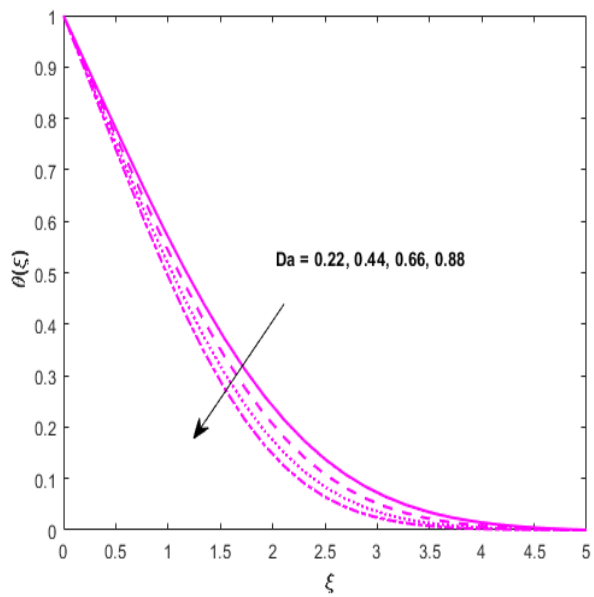


Fig. 13. Depicts the Da on $\theta(\xi)$ distribution

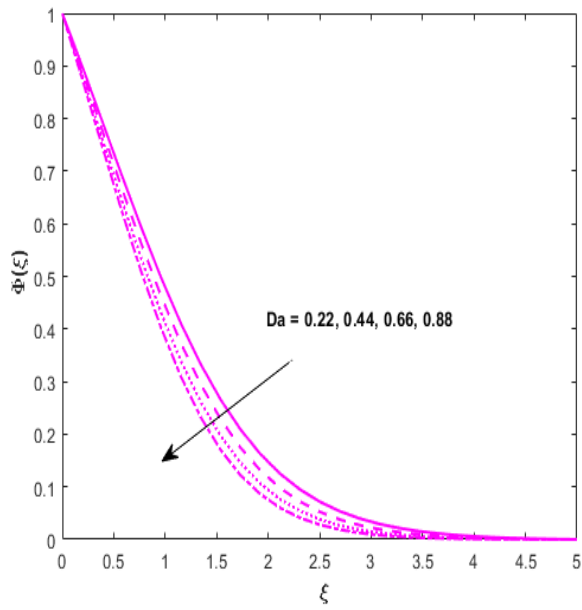


Fig. 14. Depicts the Da on $\theta(\xi)$ distribution

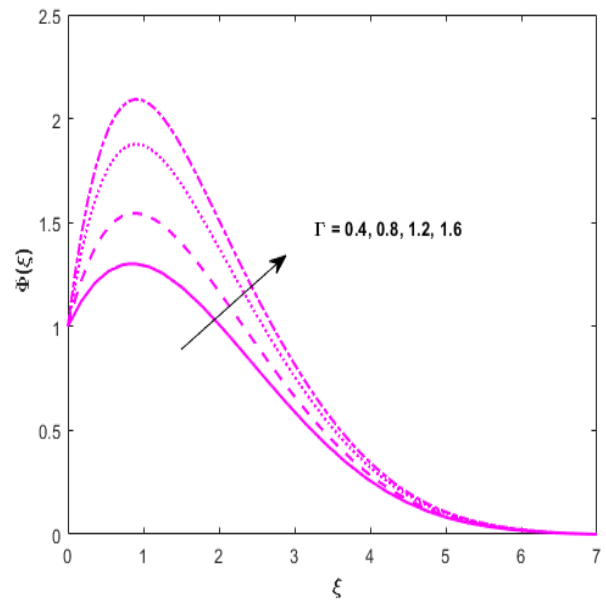


Fig. 15. Depicts the Γ on $\Phi(\xi)$ distribution

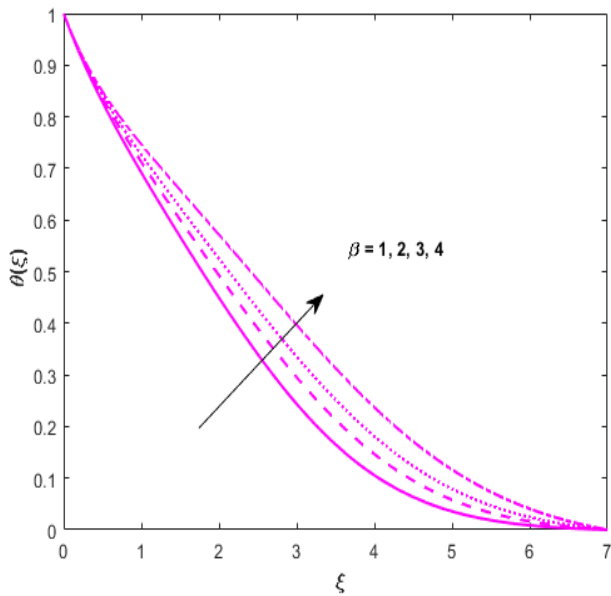


Fig. 16. Depicts the β on $\theta(\xi)$ distribution

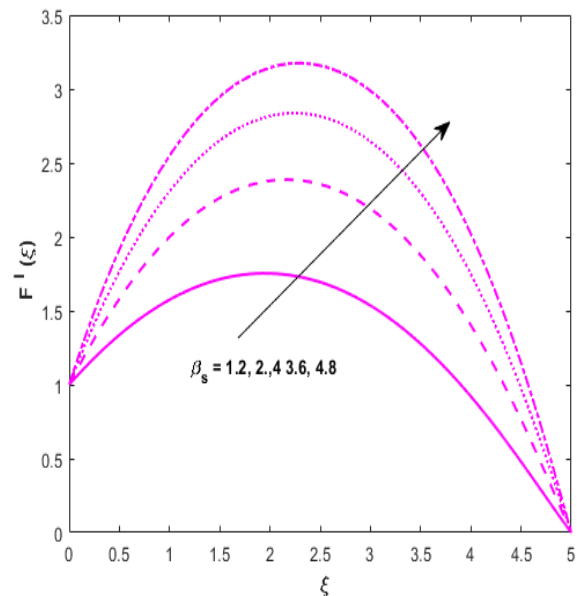


Fig. 17. Depicts the β_s on $F^I(\xi)$ distribution

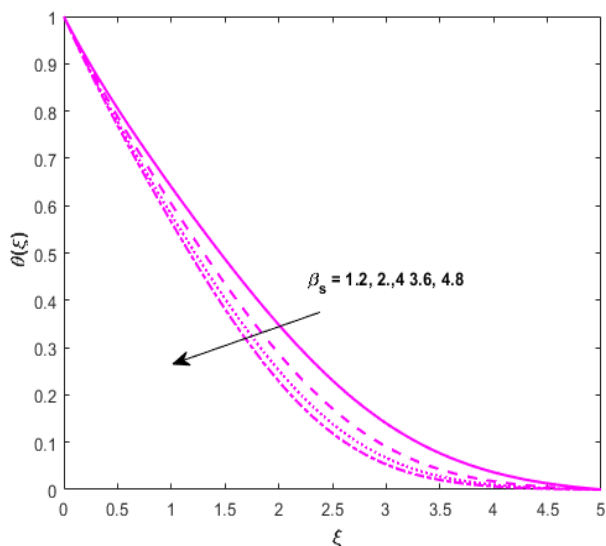


Fig. 18. Depicts the β_s on $\theta(\xi)$ distribution

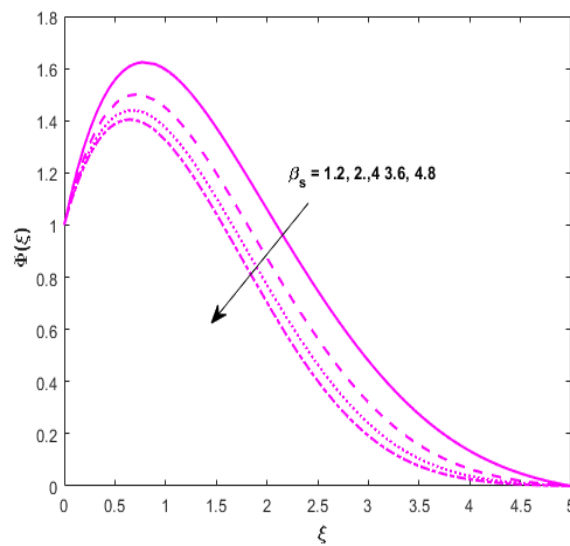


Fig. 19. Depicts the β_s on $\Phi(\xi)$ distribution

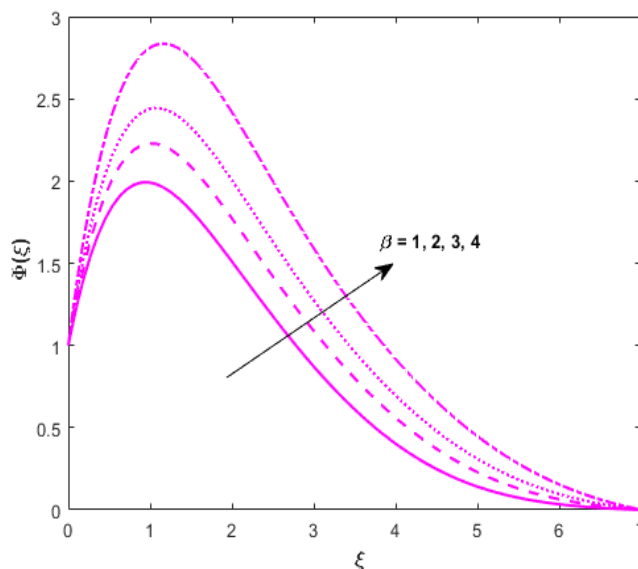


Fig. 20. Depicts the β on $\Phi(\xi)$ distribution

4. Table Comparison of Nusselt Number

Comparison of Nusselt number $\theta^1(0)$ for the case of $M = \beta = \varphi = 0$. and found an excellent agreement, as shown in Table 1. In the absence of the nano-particle volume fraction, $\phi = 0$, the problem reduces to that of Ahmad [33].

Table 1

Comparison of Nusselt number $\theta^1(0)$ for the case $M = \beta = \varphi = 0$.

Pr	Ishak [31]	Pal [32]	Present study
1.0	1.3333	1.333333	1.337049
3.0	2.5097	2.509715	2.500404
10.0	4.7969	4.796871	4.798531

5. Conclusions

The present study describes the boundary layer flow of Darcy forchheimer of MHD Jeffrey nano-fluid flow and heat transfer via a non-linear stretching sheet considering melting heat transfer and viscous dissipation. The profiles were done by taking numerical estimates of physical parameters are magnetic parameters, such as the Jeffery parameter, computation is conducted by the 4th Runge-Kutta numerical technique. The main comments of this revise are as follows:

- i. Increases in the Deborah number β result in a drop in the thickness of the momentum boundary layer and an increase in the thickness of the thermal boundary layer.
- ii. The impact of Deborah number β and parameter on the velocity is quite opposite
- iii. When the melting parameter is increased, the rate increases and the temperature decreases.
- iv. Concentration distributions decelerated with improve in melting parameter.
- v. The temperature gradient at the surface decreases when the melting parameter is increased.
- vi. The melting parameter lowers the temperature field while increasing velocity.

Conflict of interests

The authors declare that are no conflict of interests.

References:

- [1] Lee, Lawrence L. "Boundary layer over a thin needle." *The physics of fluids* 10, no. 4 (1967): 820-822. <https://doi.org/10.1063/1.1762194>
- [2] Narain, Jai Prakash, and Mahinder S. Uberoi. "Combined forced and free-convection heat transfer from vertical thin needles in a uniform stream." *The Physics of Fluids* 15, no. 11 (1972): 1879-1882. <https://doi.org/10.1063/1.1693798>
- [3] Sakiadis, Byron C. "Boundary-layer behavior on continuous solid surfaces: I. Boundary-layer equations for two-dimensional and axisymmetric flow." *AIChE Journal* 7, no. 1 (1961): 26-28. <https://doi.org/10.1002/aic.690070108>
- [4] Hayat, T., Z. Iqbal, M. Qasim, and S. Obaidat. "Steady flow of an Eyring Powell fluid over a moving surface with convective boundary conditions." *International Journal of Heat and Mass Transfer* 55, no. 7-8 (2012): 1817-1822. <https://doi.org/10.1016/j.ijheatmasstransfer.2011.10.046>
- [5] Akbar, Noreen Sher, and S. Nadeem. "Characteristics of heating scheme and mass transfer on the peristaltic flow for an Eyring-Powell fluid in an endoscope." *International Journal of Heat and Mass Transfer* 55, no. 1-3 (2012): 375-383. <https://doi.org/10.1016/j.ijheatmasstransfer.2011.09.029>
- [6] Mabood, F., S. Shateyi, M. M. Rashidi, E. Momoniat, and N. J. A. P. T. Freidoonimehr. "MHD stagnation point flow heat and mass transfer of nanofluids in porous medium with radiation, viscous dissipation and chemical reaction." *Advanced Powder Technology* 27, no. 2 (2016): 742-74. <https://doi.org/10.1016/j.apt.2016.02.033>
- [7] Hayat, T., Rija Iqbal, A. Tanveer, and A. Alsaedi. "Soret and Dufour effects in MHD peristalsis of pseudoplastic nanofluid with chemical reaction." *Journal of Molecular Liquids* 220 (2016): 693-706. <https://doi.org/10.1016/j.molliq.2016.04.123>
- [8] Krishnamurthy, M. R., B. C. Prasannakumara, B. J. Gireesha, and Rama Subba Reddy Gorla. "Effect of chemical reaction on MHD boundary layer flow and melting heat transfer of Williamson nanofluid in porous medium." *Engineering Science and Technology, an International Journal* 19, no. 1 (2016): 53-61. <https://doi.org/10.1016/j.jestch.2015.06.010>
- [9] Hayat, Tasawar, Taseer Muhammad, Sabir Ali Shehzad, Ahmed Alsaedi, and Falleh Al-Solamy. "Radiative three-dimensional flow with chemical reaction." *International Journal of Chemical Reactor Engineering* 14, no. 1 (2016): 79-91. <https://doi.org/10.1515/ijcre-2014-0179>
- [10] Hayat, T., M. Waqas, M. Ijaz Khan, and A. Alsaedi. "Impacts of constructive and destructive chemical reactions in magnetohydrodynamic (MHD) flow of Jeffrey liquid due to nonlinear radially stretched surface." *Journal of Molecular Liquids* 225 (2017): 302-310. <https://doi.org/10.1016/j.molliq.2016.11.023>

- [11] Roberts, Leonard. "On the melting of a semi-infinite body of ice placed in a hot stream of air." *Journal of Fluid Mechanics* 4, no. 5 (1958): 505-528. <https://doi.org/10.1017/S002211205800063X>
- [12] Abdel-Rahman, Reda G., M. M. Khader, and Ahmed M. Megahed. "Melting phenomenon in magneto hydrodynamics steady flow and heat transfer over a moving surface in the presence of thermal radiation." *Chinese Physics B* 22, no. 3 (2013): 030202. <https://doi.org/10.1088/1674-1056/22/3/030202>
- [13] Das, Kalidas. "Radiation and melting effects on MHD boundary layer flow over a moving surface." *Ain Shams Engineering Journal* 5, no. 4 (2014): 1207-1214. <https://doi.org/10.1016/j.asej.2014.04.008>
- [14] Hayat, Tasawar, Maria Imtiaz, and Ahmed Alsaedi. "Melting heat transfer in the MHD flow of Cu–water nanofluid with viscous dissipation and Joule heating." *Advanced Powder Technology* 27, no. 4 (2016): 1301-1308. <https://doi.org/10.1016/j.appt.2016.04.024>
- [15] Grosan, T., and I. Pop. "Forced convection boundary layer flow past nonisothermal thin needles in nanofluids." (2011): 054503. <https://doi.org/10.1115/1.4003059>
- [16] Trimbitas, Radu, Teodor Grosan, and Ioan Pop. "Mixed convection boundary layer flow along vertical thin needles in nanofluids." *International Journal of Numerical Methods for Heat & Fluid Flow* 24, no. 3 (2014): 579-594. <https://doi.org/10.1108/HFF-05-2012-0098>
- [17] Hayat, T., M. Ijaz Khan, M. Farooq, T. Yasmeen, and A. Alsaedi. "Water-carbon nanofluid flow with variable heat flux by a thin needle." *Journal of Molecular Liquids* 224 (2016): 786-791. <https://doi.org/10.1016/j.molliq.2016.10.069>
- [18] Ahmad, Rida, M. Mustafa, and S. Hina. "Buongiorno's model for fluid flow around a moving thin needle in a flowing nanofluid: A numerical study." *Chinese journal of physics* 55, no. 4 (2017): 1264-1274. <https://doi.org/10.1016/j.cjph.2017.07.004>
- [19] Majdalani, Joseph, Chong Zhou, and Christopher A. Dawson. "Two-dimensional viscous flow between slowly expanding or contracting walls with weak permeability." *Journal of Biomechanics* 35, no. 10 (2002): 1399-1403. [https://doi.org/10.1016/S0021-9290\(02\)00186-0](https://doi.org/10.1016/S0021-9290(02)00186-0)
- [20] Fakour, M., A. Vahabzadeh, D. D. Ganji, and M. Hatami. "Analytical study of micropolar fluid flow and heat transfer in a channel with permeable walls." *Journal of Molecular Liquids* 204 (2015): 198-204. <https://doi.org/10.1016/j.molliq.2015.01.040>
- [21] Hatami, M., A. Hasanpour, and D. D. Ganji. "Heat transfer study through porous fins (Si3N4 and AL) with temperature-dependent heat generation." *Energy Conversion and Management* 74 (2013): 9-16. <https://doi.org/10.1016/j.enconman.2013.04.034>
- [22] Hady, F., F. Ibrahim, H. El-Hawary, and A. Abdelhady. "Effect of Suction/Injection on Natural Convective Boundary-Layer Flow of A Nanofluid Past A Vertical Porous Plate Through A Porous Medium." *Journal of Modern Methods in Numerical Mathematics* 3, no. 1 (2012). <https://doi.org/10.20454/jmmnm.2012.169>
- [23] Zaimi, Khairy, Anuar Ishak, and Ioan Pop. "Unsteady flow due to a contracting cylinder in a nanofluid using Buongiorno's model." *International Journal of Heat and Mass Transfer* 68 (2014): 509-513. <https://doi.org/10.1016/j.ijheatmasstransfer.2013.09.047>
- [24] Chen, Chien-Hsin. "Combined effects of Joule heating and viscous dissipation on magnetohydrodynamic flow past a permeable, stretching surface with free convection and radiative heat transfer." (2010): 064503. <https://doi.org/10.1115/1.4000946>
- [25] Khan, Umar, Naveed Ahmed, and Syed Tauseef Mohyud-Din. "Influence of viscous dissipation and Joule heating on MHD bio-convection flow over a porous wedge in the presence of nanoparticles and gyrotactic microorganisms." *Springerplus* 5 (2016): 1-18. <https://doi.org/10.1186/s40064-016-3718-8>
- [26] Jaber, Khaled K. "Joule heating and viscous dissipation on effects on MHD flow over a stretching porous sheet subjected to power law heat flux in presence of heat source." *Open Journal of fluid dynamics* 6, no. 03 (2016): 156. <https://doi.org/10.4236/ojfd.2016.63013>
- [27] Rasool, Ghulam, Anum Shafiq, and Hülya Durur. "Darcy-Forchheimer relation in Magnetohydrodynamic Jeffrey nanofluid flow over stretching surface." *Discrete & Continuous Dynamical Systems-Series S* 14, no. 7 (2021). <https://doi.org/10.3934/dcdss.2020399>
- [28] Ramanuja, M., B. T. Raju, V. Nagaradhika, B. Madhusudhana Rao, P. Durgaprasad, and C. S. K. Raju. "Significance of Axisymmetric Flow of Casson Darcy Unsteady Slip Flow in a Suspension of Nanoparticles with Contracting Walls." *Journal of Nanofluids* 11, no. 3 (2022): 350-359. <https://doi.org/10.1166/jon.2022.1843>
- [29] Jiann, Lim Yeou, Sharena Mohamad Isa, Noraihan Afiqah Rawi, Ahmad Qushairi Bin Mohamad, and Sharidan Shafie. "Investigating the Effects of Wu's Slip and Smoluchowski's Slip on Hybrid TiO2/Ag Nanofluid Performance." *Journal of Advanced Research in Fluid Mechanics and Thermal Sciences* 107, no. 2 (2023): 236-252. <https://doi.org/10.37934/arfmts.107.2.236252>

- [30] Bakar, Shahirah Abu, Norihan Md Arifin, and Ioan Pop. "Mixed Convection Hybrid Nanofluid Flow past a Stagnation-Point Region with Variable Viscosity and Second-Order Slip." *Journal of Advanced Research in Micro and Nano Engineering* 12, no. 1 (2023): 1-21. <https://doi.org/10.37934/armne.12.1.121>
- [31] Pathak, Akshay Ranjan, and S. B. Kandagal. "Dynamic Characterization of Composite Liner-less tank with Geodesic-Isostrain Dome Contour." *Malaysian Journal on Composites Science and Manufacturing* 11, no. 1 (2023): 1-18.
- [32] Oltolina, Francesca, Ana Peigneux, Donato Colangelo, Nausicaa Clemente, Annarita D'Urso, Guido Valente, Guillermo R. Iglesias, Concepcion Jiménez-Lopez, and Maria Prat. "Biomimetic magnetite nanoparticles as targeted drug nanocarriers and mediators of hyperthermia in an experimental cancer model." *Cancers* 12, no. 9 (2020): 2564. <https://doi.org/10.3390/cancers12092564>
- [33] Mani, Ramanuja. "Entropy analysis of MHD flow of Jeffrey fluid in an inclined channel." *Heat Transfer* 51, no. 6 (2022): 5789-5807. <https://doi.org/10.1002/htj.22569>
- [34] Ramanuja, Mani, J. Kavitha, A. Sudhakar, A. Ajay Babu, Hari Kamala Sree, and K. Ramesh Babu. "Effect of Chemically Reactive Nanofluid Flowing Across Horizontal Cylinder: Numerical Solution." *Journal of Advanced Research in Numerical Heat Transfer* 12, no. 1 (2023): 1-17.